

Multiple Recapture of Electrons in Multiple Ionization of the Argon Dimer by a Strong Laser Field

J. Wu,^{1,2} A. Vredenburg,¹ B. Ulrich,¹ L. Ph. H. Schmidt,¹ M. Meckel,¹ S. Voss,¹ H. Sann,¹ H. Kim,¹ T. Jahnke,¹ and R. Dörner^{1,*}

¹*Institut für Kernphysik, Goethe Universität, Max-von-Laue-Strasse 1, D-60438 Frankfurt, Germany*

²*State Key Laboratory of Precision Spectroscopy, East China Normal University, Shanghai 200062, China*

(Received 5 April 2011; published 20 July 2011)

We observe multiply frustrated tunneling ionization-induced dissociation of the argon dimers by intense linearly polarized ultrashort laser pulses. By measuring the kinetic energy release and angular distribution of the Coulomb explosion of up to eightfold ionized argon dimers, we can trace the recapture of up to two electrons to Rydberg states of the highly charged compound at the end of the laser pulse. Upon dissociation of the dimer, the Rydberg electron prefers to localize at the atomic ion with the higher charge state. We probe the electron recapture dynamics by a time-delayed weak pulse.

DOI: 10.1103/PhysRevLett.107.043003

PACS numbers: 32.80.Rm, 42.50.Hz, 42.65.Re

Electrons set free from an atom or molecule by a strong laser field perform a driven oscillatory motion. This motion gives rise to a wealth of fascinating phenomena [1], such as high harmonic generation [2], electron impact ionization and excitation [3,4], or elastic scattering [5] and diffraction [6]. Recently, it was demonstrated that the quivering electron can be trapped into a high lying Rydberg state at the end of the laser pulse [7–19], leading to highly excited neutral atoms or singly charged ions. In the present work we show the influence of this mechanism in the production of highly charged ions and observe that more than one electron can be recaptured.

We use the argon dimer (Ar_2) as a model system to gain insight into the dynamics of the multiple ionization process and the electron recapture. We exploit that Ar_2 introduces two different time and length scales into the process of multiple ionization. These are, namely, the short time of the ionization processes versus the much longer time for Coulomb explosion (CE) of the system and the large size of the Rydberg orbitals (typically ~ 150 a.u.) versus the much smaller internuclear distance of the ground state dimer ($R_e \sim 7.1$ a.u.) [20]. The laser pulse and hence the forced electron motion terminate after about 35 fs. During that time multiple electrons are ejected from either site of the Ar_2 forming an initial (Ar^{p+} , Ar^{q+}) dimer ion. Those electrons which are trapped form Rydberg orbitals significantly larger than the internuclear distance of Ar_2 . In a second step, the highly charged (Ar^{p+} , Ar^{q+}) atoms within the cloud of Rydberg electrons start moving apart; i.e., the dimer Coulomb explodes. This explosion is initially driven by the full charges p and q , unscreened of the Rydberg electrons. Only later, when the system has expanded to the size of the Rydberg orbitals, the electrons start to screen the charges and eventually the Rydberg electrons localize at one or the other ion forming the final $\text{Ar}^{n+} + \text{Ar}^{m+}$ which we detect [labeled as $\text{Ar}(n, m)$]. As we will show in the following, the initial charges as well as the distance at which the

electrons start to shield are encoded in the kinetic energy of the ionic fragments. Thus, measuring the kinetic energy release (KER), the final charges (n, m) and the angular distribution of the two ions give detailed insight into the role of electron recapture in strong field multiple ionization. We find that the electron recapture probability strongly depends on the intermediate charge state and dimer orientation. We probe the dynamics by stripping off the Rydberg electron with a time-delayed weak pulse. Experimentally, the Ar_2 from the supersonic gas jet is multiply ionized by femtosecond laser pulses (35 fs, 790 nm, 8 kHz) and measured with a standard cold target recoil ion momentum spectroscopy (COLTRIMS) setup [21].

Figure 1(a) shows the measured KER distribution of the multiply ionized Ar_2 by using linearly polarized pulses with a peak intensity of $I_0 \sim 8 \times 10^{14}$ W/cm². Different dissociation channels from $\text{Ar}(1, 1)$ to $\text{Ar}(4, 3)$ were observed. The charge symmetric channel is produced much more efficiently than the charge asymmetric one. This is in contrast to the ionization by a projectile ion [22]. For instance, for Ar_2^{4+} , the yield ratio of $\text{Ar}(2, 2)$ ($\sim 21.36\%$) is much higher than $\text{Ar}(3, 1)$ ($\sim 0.26\%$) (see Table I). This agrees with the fact that $\text{Ar}(3, 1)$ is much more difficult to access due to its higher potential energy curve [22]. For Ar_2^{6+} , we observe only the charge symmetric channel $\text{Ar}(3, 3)$ and none of the possible charge asymmetric ones [e.g., $\text{Ar}(4, 2)$].

Interestingly, as shown in Fig. 1(a), there are several distinct KER peaks for all the observed dissociation channels. For each detected charge state (n, m), the most prominent peak is at $\text{KER} \sim (n \times m)/R_e$, resulting from the direct CE of the (Ar^{n+} , Ar^{m+}) pair. We also observe additional maxima at higher KER, which are not present for circularly polarized light. This clearly indicates that the higher KER peaks are related to the return of the electron (s) to their parent ion (recollision), which is absent for circular light. The additional peaks at higher KER are close

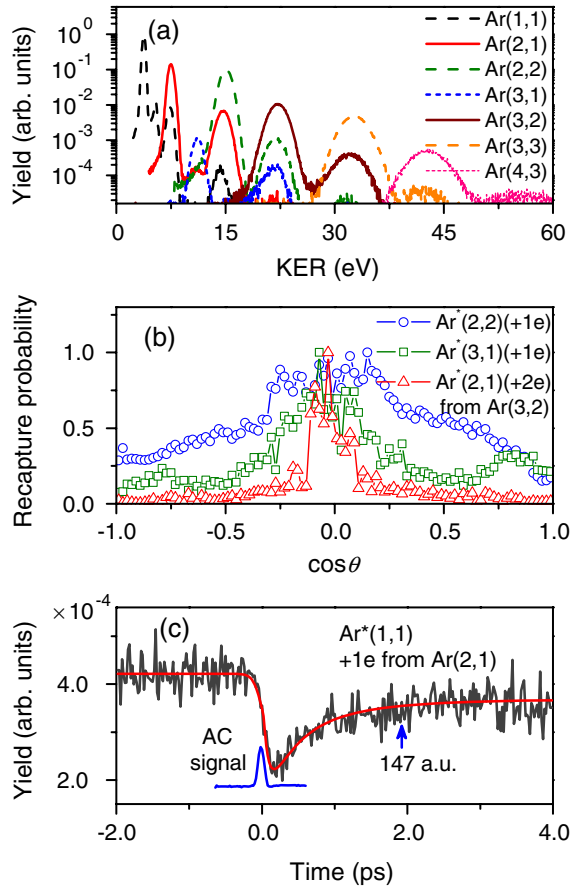


FIG. 1 (color online). (a) The KER distribution of multiple ionization-induced dissociation channels of Ar_2 by using linearly polarized laser pulse. (b) The normalized recapture probability as function of angle between the laser field polarization and dimer axis. The probability is the ratio of the detected electron recapture channel and all the channels with same initial charge state. (c) The pump-probe time dependent yield of the one electron recapture channel $\text{Ar}^*(1,1)$. The positive time delay indicates the probe pulse comes later than the pump one. The blue curve represents the autocorrelation (AC) signal of the pulses.

to those of higher charge states. While the final charge states are (n, m) , the KER seems to stem from CE of some higher initial charges (p, q) , which can be directly identified via the KER.

In the following we will use the information to first learn about the recapture mechanism itself and then how the Rydberg electron localizes at one or the other core as the dimer dissociates.

What is the probability of recapturing one or more electrons and how does it depend on the charge state? Figure 2(a) compares our measured charge state dependence of the recapture probability with theoretical predictions [see Eq. (14) in Ref. [16]]. Here, by assuming tunneling around the pulse peak, the electron trapping probability approximates to $1/(1 + \Gamma)$, where $\Gamma = 0.5\pi E_0^{3/2} \omega_0^{-1} \tau^{2/3} (2I_p)^{-1/4} (4Q)^{-2/3} (1 - 0.5QE_0I_p^{-2})$, τ , ω_0 , and E_0 are the duration, carrier frequency, and

TABLE I. The yield ratio and electron recapture probability of the multiple ionization-induced dissociation channels of Ar_2 . The yield ratio is normalized to the total counts of the observed dissociation channels. The electron recapture probability is estimated by normalizing the yield of the electron recapture channel to the total yield of all the channels with the same initial charge state.

Dissociation channels	Ratio (%)	Recapture probability (%)
Ar(1, 1): 3.8 eV	53.88	
Ar(1, 1): 5.3 eV	0.93	
Ar*(1, 1): 7.3 eV	0.95	6.02 [+ 1e from Ar(2, 1)]
Ar*(1, 1): 14.3 eV	0.03	0.13 [+ 2e from Ar(2, 2)]
Ar(2, 1): 7.5 eV	14.82	
Ar*(2, 1): 10.9 eV	0.05	20.0 [+ 1e from Ar(3, 1)]
Ar*(2, 1): 14.7 eV	1.51	6.70 [+ 1e from Ar(2, 2)]
Ar*(2, 1): 21.7 eV	0.01	0.26 [+ 2e from Ar(3, 2)]
Ar(2, 2): 15.1 eV	21.00	
Ar*(2, 2): 21.9 eV	0.35	9.21 [+ 1e from Ar(3, 2)]
Ar*(2, 2): 31.7 eV	0.01	0.41 [+ 2e from Ar(3, 3)]
Ar(3, 1): 11.1 eV	0.20	
Ar*(3, 1): 21.6 eV	0.06	1.58 [+ 1e from Ar(3, 2)]
Ar(3, 2): 22.2 eV	3.38	
Ar*(3, 2): 32.0 eV	0.21	8.54 [+ 1e from Ar(3, 3)]
Ar(3, 3): 32.7 eV	2.24	
Ar*(3, 3): 42.0 eV	0.02	5.88 [+ 1e from Ar(4, 3)]
Ar(4, 3): 42.8 eV	0.32	
Ar*(4, 3): 55.6 eV	0.03	— [+ 1e from Ar(4, 4)]

amplitude of the laser pulse, I_p is the ionization potential of the dimer ion from $\text{Ar}_2^{(Q-1)+}$ to Ar_2^{Q+} . We find probabilities for recapturing one electron in the range of 6%–12% depending on the intermediate charge state $Q = (p + q)$, which is comparable or more probable than the well-studied strong field effects [2–6].

We also observe recapture of two electrons. As shown in Fig. 1(a), under the most prominent KER peak of Ar(2, 2), there is a small peak belonging to the $\text{Ar}^*(1,1)$ channel at 14.3 eV, which results from the recapture of two electrons to the ion pair of $(\text{Ar}^{2+}, \text{Ar}^{2+})$, one at each nucleus. One might find it surprising that double Rydberg states are formed as they are continuum states and can decay by autoionization. Their survival indicates that the trapped two electrons mostly distribute at the opposite sides of the Rydberg orbital, which can survive as the avoided collision reduces autoionization [23]. Very small KER peaks are also observed for the $\text{Ar}^*(2,1)$ and $\text{Ar}^*(2,2)$ channels at 21.7 and 31.7 eV, respectively, which come from the two-electron recapture of Ar(3, 2) and Ar(3, 3).

It is predicted that from all ionized electrons only those are recaptured which have tunneled very close to the electric field maximum [11,12,15,16]. Our data allow us to test this prediction by exploring the dependence of the recapture probability on the orientation of the dimer axis to the laser field. The Ar_2 is ionized more easily if oriented

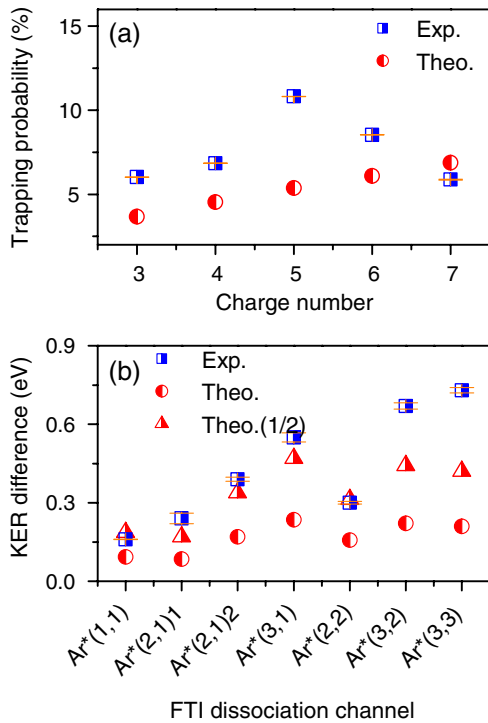


FIG. 2 (color online). (a) The electron trapping probability as a function of the intermediate state charge number Q . (b) The KER difference between the one electron recapture channel and the corresponding parent fragment pair. $Ar^*(2, 1)1$ and $Ar^*(2, 1)2$ denote the one electron recapture channels from the $Ar(3, 1)$ and $Ar(2, 2)$, respectively. The circles and triangles represent the theoretical values obtained for the full size of the Rydberg orbital and half of its size, respectively.

parallel to the field [18,19]. For Ar_2 with axis parallel to the strong field, the electron tunneling may occur much before the extrema of the individual laser cycles or earlier in the laser pulse rising edge. These electrons with a certain amount of kinetic energies will escape from the Coulomb potential of the ionic core. However, for Ar_2 orthogonal to the field, the electron tunneling occurs only in a very narrow time interval around the laser field extrema. This electron with negligible drift kinetic energy at the end of the laser pulse shows a high recapture probability. The measured angular distributions of the recapture probability shown in Fig. 1(b) adequately verify this expectation. Obviously, the electron recapture probability is higher for the dimers orientated orthogonally to the field, which is more significant for the two-electron recapture channel. In addition, the different angular distributions of the $Ar^*(2, 2)$ and $Ar^*(3, 1)$ indicate the important role of the electron localization step. For the weak spectrometer field of 7.5 V/cm, we estimate that only a Rydberg electron with principal quantum number $\langle n \rangle > 80$ can be field ionized, which is much higher than the Rydberg states considered in this work and hence should have negligible influence.

All KER peaks associated with recapture of an electron are slightly shifted to smaller KER compared to the same

peak without recapture [see Fig. 1(a)]. This shift contains information on the size of the Rydberg orbital. It is shown in Fig. 2(b) together with an estimate for a lower bound of this shift obtained from a simple model. Following Ref. [16], we estimate the orbital radius of the Rydberg electron tunneled around the laser pulse peak to $\langle r \rangle = (0.5Q\tau^2)^{1/3}$, which agrees well with the Monte Carlo and quantum mechanical simulations [11,16]. For our pulse duration of $\tau = 35$ fs, the orbital radius of the trapped Rydberg electron ranges from $\langle r \rangle = 146$ to 194 a.u. for Ar_2^{Q+} with Q ranging from 3 to 7. Correspondingly, the principal quantum number $\langle n \rangle = (2Q\langle r \rangle/3)^{1/2}$ [19] and the Kepler period $\langle T_k \rangle = 2\pi\langle n \rangle^3/Q^2$ [10] are estimated to range from $\langle n \rangle = 17$ to 30 and $\langle T_k \rangle \sim 85$ fs, respectively. The dimer ion Ar_2^{Q+} inside the Rydberg orbital then dissociates along the Coulomb repulsive potential curve of (Ar^{p+}, Ar^{q+}) . The trapped Rydberg electron might localize at one of the nuclei when they approach the Rydberg orbital $\langle r \rangle$. Therefore, we assume that the fragments jump from the potential energy curve of (Ar^{p+}, Ar^{q+}) to (Ar^{m++}, Ar^{q+}) at an internuclear distance of twice the radius of the Rydberg orbital. The sudden localization of the Rydberg electron to one of the nuclei shields the charge of the latter, making the KER of the detected $Ar^*(m, q)$ channel slightly smaller than its parent intermediate channel $Ar(p, q)$. This estimate gives only an upper bound for the internuclear distance from where the recaptured electron will start to screen the charges (p, q) . As the Rydberg states are expected to be elliptical with angular momentum $l > 0$, the effective radius is likely to be smaller. Figure 2(b) shows the expected KER differences of the electron recapture dissociation channels for the maximum size of the Rydberg orbital and half of its size. This reduced value shows reasonable agreement with the experimental results, indicating a high l state of the trapped Rydberg electron.

In the following we will now further discuss the fate of the Rydberg electron during the dissociation. To address this directly we probed the Rydberg electron by using an additional time-delayed parallel polarized weak fs pulse ($I_0 \sim 1 \times 10^{14}$ W/cm²). This pulse ionizes the Rydberg electron and eventually decreases the electron recapture probability. Taking the one electron recapture channel $Ar^*(1, 1)$ from $Ar(2, 1)$ as an example, Fig. 1(c) nicely shows the electron recapture dynamics. As marked with the arrow, the yield is almost constant after ~ 1.9 ps, which corresponds to an internuclear distance of ~ 147 a.u.. At this time the Rydberg electron is localized to one of the dissociating nuclei. This corresponds to a principal quantum number $\langle n \rangle \sim 17$, and agrees well with the classical prediction for $Q = 3$ as discussed above. The blue curve in Fig. 1(c) shows the autocorrelation signal of the pulses. Obviously, the electron recapture channel is maximally depleted when the probe pulse is coming around the end of the pump one, which speeds up the tunneled electron and stops its trapping to the Rydberg orbital.

For more asymmetric channels it is also interesting to see at which of the two nuclei the Rydberg electron will localize. For the Ar(2, 1) channel, as shown in Fig. 1(a), there are two high KER peaks at 10.9 and 14.7 eV which are produced by one electron recapture of Ar(3, 1) and Ar(2, 2), respectively. As listed in Table I, the recapture probability to produce Ar*(2, 1) is much higher for Ar(3, 1) ($\sim 20\%$) than Ar(2, 2) ($\sim 6.7\%$). Another example is the initial pair (Ar³⁺, Ar²⁺). Here a recaptured electron can localize at the nuclear core of either Ar³⁺ or Ar²⁺, leading to the recapture channels of Ar*(2, 2) and Ar*(3, 1), respectively. We find the one electron recapture probability to produce Ar*(2, 2) ($\sim 9.21\%$) is much higher than the one to produce Ar*(3, 1) ($\sim 1.58\%$). It indicates that, after the first step of tunneling ionization and trapping by the Coulomb potential of the molecular ion, the localization of the Rydberg electron occurs preferably at the nuclear with the higher charge state.

In summary, we have shown that recapture of electrons is very general in strong laser field multiple ionization. We have measured the recapture probability and its dependence on the charge state directly. The dissociation dynamics of the Ar₂ also allow us to follow the decay of the Rydberg state in time as the highly charged two ions inside the orbit dissociate. Our measured strong angular distribution of the recapture probability experimentally supports that the recapture probability is highest for electrons born at the field maximum.

J. W. acknowledges support by the Alexander von Humboldt Foundation. Support by a Koselleck Project of the Deutsche Forschungsgemeinschaft is acknowledged.

*doerner@atom.uni-frankfurt.de

- [1] P. B. Corkum, *Phys. Rev. Lett.* **71**, 1994 (1993).
- [2] M. Drescher *et al.*, *Science* **291**, 1923 (2001).
- [3] B. Walker *et al.*, *Phys. Rev. Lett.* **73**, 1227 (1994).
- [4] R. Dörner *et al.*, *Adv. At. Mol. Opt. Phys.* **48**, 1 (2002); A. Becker, R. Dörner, and R. Moshammer, *J. Phys. B* **38**, S753 (2005).
- [5] Z. Chen *et al.*, *Phys. Rev. A* **79**, 033409 (2009).
- [6] M. Meckel *et al.*, *Science* **320**, 1478 (2008).
- [7] M. P. de Boer and H. G. Muller, *Phys. Rev. Lett.* **68**, 2747 (1992).
- [8] R. R. Jones, D. W. Schumacher, and P. H. Bucksbaum, *Phys. Rev. A* **47**, R49 (1993).
- [9] G. L. Yudin and M. Yu. Ivanov, *Phys. Rev. A* **63**, 033404 (2001).
- [10] E. Wells, I. Ben-Itzhak, and R. R. Jones, *Phys. Rev. Lett.* **93**, 023001 (2004).
- [11] T. Nubbemeyer *et al.*, *Phys. Rev. Lett.* **101**, 233001 (2008).
- [12] U. Eichmann *et al.*, *Nature (London)* **461**, 1261 (2009).
- [13] B. Manschwetus *et al.*, *Phys. Rev. Lett.* **102**, 113002 (2009).
- [14] T. Nubbemeyer, U. Eichmann, and W. Sandner, *J. Phys. B* **42**, 134010 (2009).
- [15] K. N. Shomsky, Z. S. Smith, and S. L. Haan, *Phys. Rev. A* **79**, 061402(R) (2009).
- [16] N. I. Shvetsov-Shilovski *et al.*, *Laser Phys.* **19**, 1550 (2009).
- [17] I. A. Burenkov *et al.*, *Laser Phys. Lett.* **7**, 409 (2010).
- [18] B. Ulrich *et al.*, *Phys. Rev. A* **82**, 013412 (2010).
- [19] B. Manschwetus *et al.*, *Phys. Rev. A* **82**, 013413 (2010).
- [20] K. Patkowski *et al.*, *Mol. Phys.* **103**, 2031 (2005).
- [21] R. Dörner *et al.*, *Phys. Rep.* **330**, 95 (2000).
- [22] J. Matsumoto *et al.*, *Phys. Rev. Lett.* **105**, 263202 (2010).
- [23] S. N. Pisharody and R. R. Jones, *Science* **303**, 813 (2004).